Probabilistic Engineering Mechanics 84 (2026) 103923

Contents lists available at ScienceDirect

Probabilistic Engineering Mechanics

journal homepage: www.elsevier.com/locate/probengmech

Crossing-consistent peak count The most conservative crossing-consistent cycle count

Wim Bierbooms

Wind Energy, Faculty of Aerospace Engineering, Delft University of Technology, Kluyverweg 1, 2629 HS, Delft, the Netherlands

ARTICLE INFO

Keywords:
Peak count
Crossing consistency
Cycle count
Upper bound
Fatigue
Wind turbine loads
Narrow-band approximation

ABSTRACT

This study introduces a new variant of the peak count, termed the crossing-consistent peak count. Crossing consistency implies that the number of cycles with peaks above and valleys below a certain level equals the number of up-crossings of that level. The conventional peak count does not exhibit crossing consistency. In the crossing-consistent peak count, valleys are paired with the nearest peaks, from the largest to the smallest, and each cycle is counted as a full cycle. To include half cycles, the reversals of the time series are considered twice, except for the start and end points, such that each cycle is counted as a half cycle. Based on the fatigue framework developed by the Lund University, in which the cumulative cycle histogram is a key element, this study shows that the crossing-consistent peak count is the most conservative crossing-consistent counting method. This holds true for all time series, not only Gaussian signals. The crossing-consistent peak count was applied to wind turbine loads and compared with the rainflow count and conventional peak count. Moreover, it was applied to broad-band Gaussian signals, and it was concluded that the mean damage follows the narrow-band approximation.

1. Introduction

This paper addresses, cycle counting, which is a crucial step in fatigue analysis. In a typical time-domain fatigue analysis, simulations are first performed to estimate the internal loads. Then, based on these loads, the stress values are established. Next, the stress cycles are determined, based on which, the fatigue damage is calculated using an *S–N* curve and the Palmgren–Miner summation rule. In particular, the stress cycles are determined through two stages. First, the reversals (peaks and valleys) are extracted from the time series, and second, the identified peaks are paired with the valleys. The cycle-counting method determines how this pairing is performed, that is, which peak is paired with which valley. The estimated damage is influenced by multiple factors, including the length and sampling rate of the time series and the subsequent filtering. Because the current study is focused only on cycle counting, it does not examine these factors.

Thus, the reversals (turning points) of a stress time series serve as the starting point of this study. The lifetime of the structure can be calculated by simulating the damage caused by each load. Furthermore, because the lifetime is also a random variable, generally, the expected value of damage is considered. In time domain, this value is obtained by averaging the damages from repeated load simulations under the same environmental conditions. If the stress is known to be Gaussian, readily available analytical expressions can be used for estimating the expected damage. This also enables researchers to perform simulations in the frequency domain because if the excitation is Gaussian (such as a turbulent wind field or random sea waves), the response of a linear system will also be Gaussian. From the moments of the stress spectrum, the average damage can be straightforwardly derived [1]. The expected damage per time instant obtained via the frequency domain approach is equivalent to the average damage per time instant determined from an infinitely long time series. This implies that the results of frequency domain techniques are valid for infinitely long time series only. It should be noted that the scope of this paper is limited to finite time series from an arbitrary stochastic process.

Next, three well known counting methods are introduced. In the range count, successive peaks and valleys (crest to trough) are paired to form half cycles. Instead of specifying the stress ranges of the counting method, this study plots the scatter diagram shown in Fig. 1b. This approach, in addition to providing a clear way to present the counting method, also serves a mathematical purpose, as will become evident in Section 2. In the conventional peak count, the highest positive peak and the lowest negative valley are paired, followed by the second-highest positive peak and the second-lowest negative valley, and so on. Therefore, this count method results only in full cycles (see Fig. 1c). The rainflow count is regarded as the most optimal counting method and has

E-mail address: w.a.a.m.bierbooms@tudelft.nl.

https://doi.org/10.1016/j.probengmech.2026.103923
Received 6 October 2025; Received in revised form 13 March 2026; Accepted 25 March 2026
Available online 1 April 2026

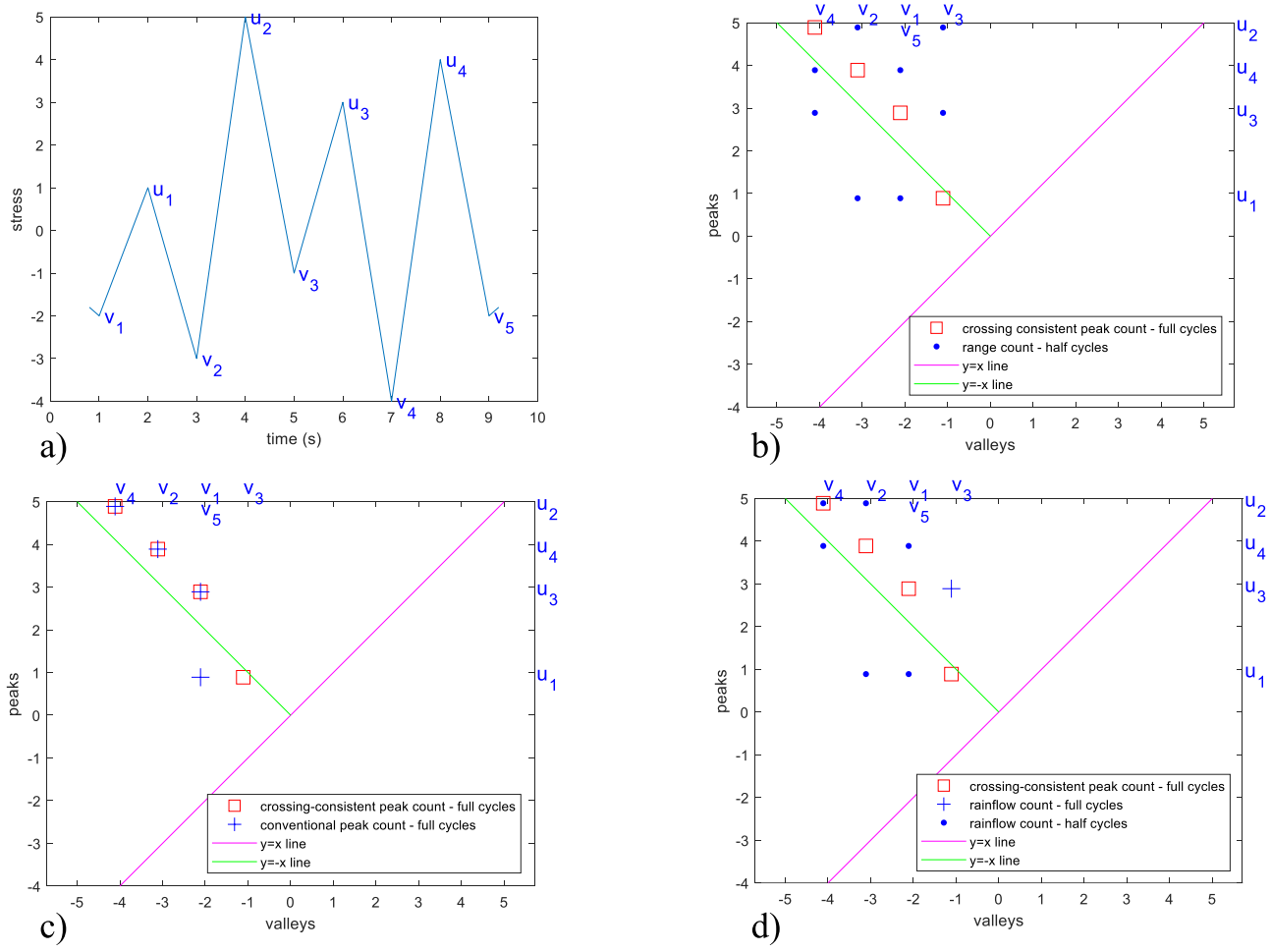

Fig. 1. a) An example time series of a stress, b) scatter diagram of the range count cycles compared with the crossing-consistent peak count, c) idem for the conventional peak count cycles and d) idem for the rainflow count cycles.

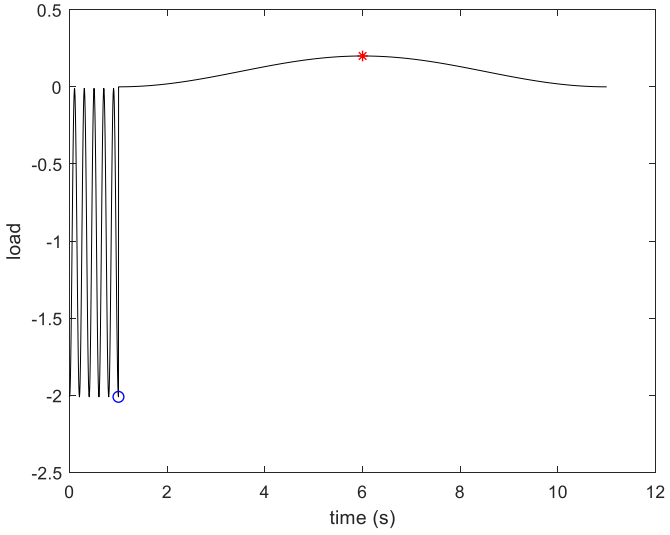

Fig. 2. An example time series of a load with just one positive peak (indicated in red). (For interpretation of the references to colour in this figure legend, the reader is referred to the Web version of this article.)

been studied extensively [2,3]. It results into half as well as full cycles, see Fig. 1d.

This paper proposes a counting method referred to as the crossing-consistent peak count. Crossing consistency implies that all peaks and valleys are paired. This is generally not the case in the conventional peak count. In the crossing-consistent peak count, each valley (from large to small) is paired with the nearest peak above it. Based on this description, one may question whether this approach will lead to the highest fatigue damage. However, as proven later in Section 4, it is apparently the most conservative cycle count. The core concept is that the smaller peaks are paired with the larger valleys, leaving the larger peaks to the smaller valleys, ultimately leading to large ranges. Fig. 1 compares this counting method with the introduced counting methods.

The conventional peak count is generally considered the most conservative. The ASTM standard [4], states (Section 5.2), without proof or reference, that '*Peaks above the reference load level are counted, and valleys below the reference load level are counted …. The most damaging cycle count for fatigue analysis is derived from the peak count by first constructing the largest possible cycle, using the highest peak and lowest valley, followed by the second largest cycle, etc., until all peak counts are used*'. Fig. 2 shows a load time series with zero mean; it consists of five cycles (just below zero) and one small, slow cycle. Because this time series has a single positive peak, it is obvious that the peak count, as described above, will not be the most damaging cycle count, which contradicts the ASTM statement.

This work has been inspired by the intriguing quote from Ref. [5]: '*Observe that one can always construct a crossing consistent cycle count with distribution N(x,y)=K(x,y), i.e. the most conservative cycle count, but we*

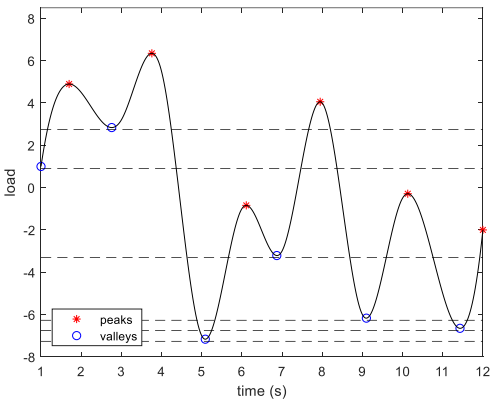

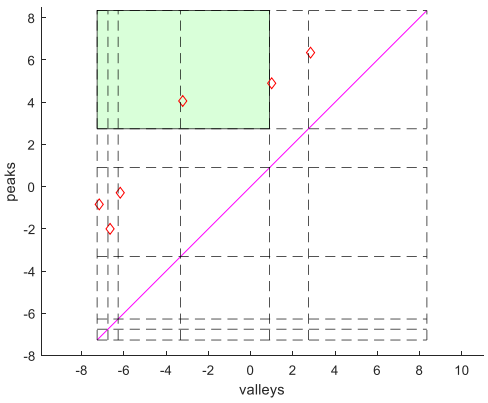

0	0	0	1	2	3
0	0	0	1	2	-
1	2	3	4	-	-
1	2	3	-	-	-
1	2	-	-	-	-
1	-	-	-	-	-

Fig. 3. a) An example time series of a load, b) scatter plot of the range count cycles, and c) the corresponding cumulative histogram *N(u,v)*.

shall not discuss this further here'. To the best of author's knowledge, this cycle count has never been explicitly addressed to date despite being the most conservative. Succeeding sections show that the proposed crossing-consistent peak count turns out to be the specific cycle count referred to in the above quote.

The crossing-consistent peak count is further detailed in Section 3. Section 4 demonstrates that the damage based on the crossing-consistent peak count is the upper bound of the damage of any stress (not restricted to the Gaussian signals) for all crossing-consistent cycle counts, including the rainflow count. This evidence is based on a fatigue framework developed at the Lund University. This framework is explained in Section 2. In Section 5, the crossing-consistent peak count is applied to several real-life time series and is compared with the rainflow count.

This study adopts the standard terminology given in Ref. [4]. Therefore, a local maximum (crest) is indicated here by a peak and a local minimum (trough) by a valley. Thus, a cycle refers to a peak–valley pair.

2. Fatigue framework used in this study

This section details the fatigue framework used in this study [5–7]. It should be noted that, in this section (and Section 3), only full cycles are considered in accordance with this framework. General cases, including half cycles, are discussed in Section 4.

Fig. 3a shows an example load time series with different load levels. Every cycle-counting method pairs a specific peak u to some specific valley v. This is conveniently displayed by a scatter plot presented in Fig. 3b. As shown in this illustration, the positive range count cycles and, thus, the ranges from valleys to peaks, are counted as full cycles [4]. Because, for every cycle, the peak should be larger than or equal to the valley, all cycles are displayed above the diagonal. The stress range of each cycle, S=u-v, equals the horizontal or vertical distance to this diagonal. A key element of this framework is the cumulative histogram $N(u,v)$ (see Fig. 3c). $N(u,v)$ denotes the total number of cycles with a peak higher than u and a valley lower than v. For instance, all cycles to be counted for $N(u=2.7,v=0.9)$, i.e., the green shaded cell in Fig. 3c, is in Fig. 3b indicated by the green shaded area. From this definition, it follows that N increases monotonically from left to right in a row and from top to bottom in a column. This implies that $N(u,v) \le N(u,u)$ as well as $N(u,v) \le N(v,v)$. In fact, $N(u,v) \le N(z,z)$ where z lies between v and u. Only the upper triangle of $N(u,v)$ is shown since the lower triangle is irrelevant for the fatigue damage. This is further explained below.

The number of up-crossings N_u, of the six indicated levels (from high to low) are respectively 2, 1, 3, 2, 1, and 0. Ref. [5] specifies that a natural requirement for a counting method is that $N(u,u)$, i.e., the number of cycles with the peak above and the valley below u, equals the number of up-crossings N_u. This criterion is referred to as crossing consistency. In other words, the range count is crossing-consistent as the values of $N(u,u)$, as shown in red on the super-diagonal in Fig. 3c, are (from top to bottom) 2, 1, 3, 2, and 1.

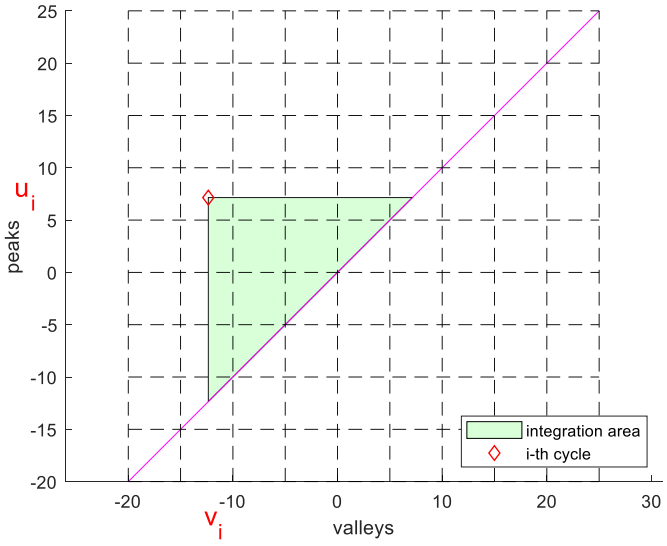

Fig. 4. Curve for the ith cycle. Area for $N(u,v) = 1$ is indicated in green, and $N(u,v) = 0$ elsewhere. (For interpretation of the references to colour in this figure legend, the reader is referred to the Web version of this article.)

The common expression for fatigue damage reads the following:

$$D = \frac{1}{K}\sum_{i=1}^{N} S_i^m, \tag{1}$$

where S_i denotes the stress range of the ith cycle, m represents the slope of the S–N curve, and K denotes a constant; $NS^m = K$. In terms of the cumulative histogram $N(u,v)$, the relation (for $m > 1$) is given by Eq. (2) (see page 6 of [6]):

$$D = \frac{m(m-1)}{K}\iint N(u,v)\,(u-v)^{m-2}\,du\,dv. \tag{2}$$

The integral bounds should be taken such that all cycles are covered. For the ith cycle we have the following (see also Fig. 4):

$$D_i = \frac{m(m-1)}{K}\int_{v_i}^{u_i}\int_{v}^{u_i}(u-v)^{m-2}\,du\,dv. \tag{3}$$

The inner integral can be evaluated as follows:

$$\int_{v}^{u_i}(u-v)^{m-2}\,du = \frac{1}{m-1}(u-v)^{m-1}\Big|_{v}^{u_i} = \frac{1}{m-1}(u_i-v)^{m-1}. \tag{4}$$

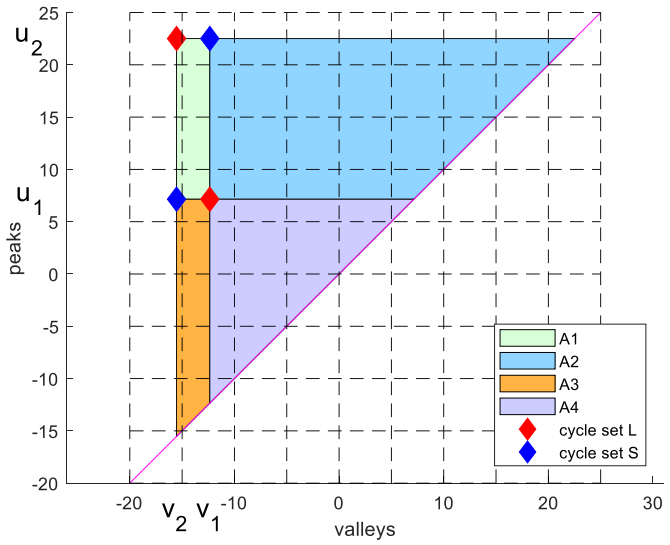

Fig. 5. Comparing the fatigue damage of two cycle sets.

Section 4.

Because $(u-v)^{m-2} \geq 0$, the damage of a crossing-consistent cycle count is bounded by the following:

$$D = \frac{m(m-1)}{K} \iint K(u,v)\,(u-v)^{m-2}\,du\,dv, \tag{6}$$

where

$$K(u,v) = \min N(z,z) = \min N_z, \tag{7}$$

and z lies between v and u.

To measure the expected damage for an infinitely long time series, an expression similar to Eq. (2) is valid with the cumulative histogram replaced by the distribution function. The Appendix details the narrow-band approximation for Gaussian loads. Furthermore, Rychlik [7] proved that, for Gaussian loads, this narrow-band approximation is the upper bound of the expected damage at any crossing-consistent count.

This study does not consider the average damage, but is focused on the damage of some given finite time series. In Section 3, a novel counting method is be presented. Section 4 presents proof that the proposed method is the most conservative and crossing-consistent cycle

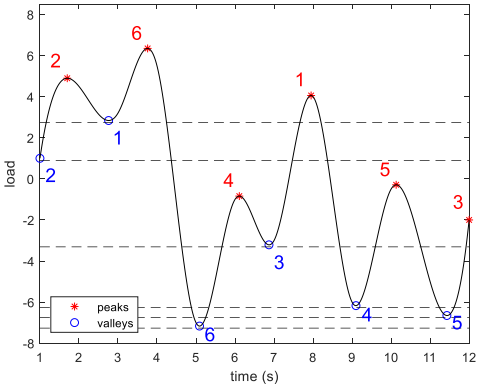

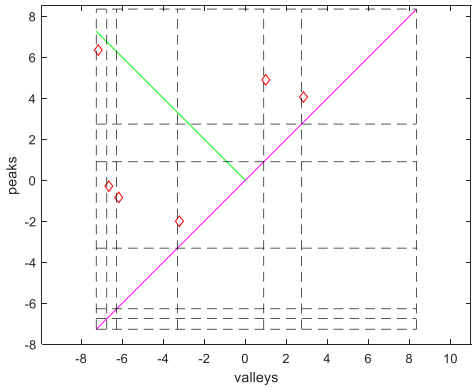

1	1	1	1	2	3
1	1	1	1	2	-
1	2	3	4	-	-
1	2	3	-	-	-
1	2	-	-	-	-
1	-	-	-	-	-

Fig. 6. a) An example time series of a load (same as Fig. 3a), b) scatter plot of the crossing-consistent peak count cycles, and c) the corresponding cumulative histogram $N(u,v)$.

Substitution in Eq. (3) results into the following:

$$D_i = \frac{m}{K}\int_{v_i}^{u_i} (u_i - v)^{m-1}\,dv = -\frac{1}{K}(u_i - v)^m\Big|_{v_i}^{u_i} = \frac{1}{K}(u_i - v_i)^m = \frac{1}{K}S_i{}^m. \tag{5}$$

Because integral addition is associative and commutative, the total damage of all cycles can be expressed as Eq. (1). Due to practical limitations, only six levels have been considered in the example plotted in Fig. 3. More levels can be utilised to obtain a finer grid. This way, the contribution of the diagonal elements $N(u,u)$ will become negligible as their range u–v approaches zero.

In practice, Eq. (2) is not preferrable over Eq. (1) [6]. However, Eq. (2) allows comparison of the damage measured by different cycle-counting methods as well as the determination of an upper bound.

An example of a comparison is shown in Fig. 5. In particular, two peaks and two valleys were assumed. These can be combined in two different ways, denoted by sets L and S. Notably, the sum of the two ranges of cycle set L equals the sum of the those of set S. For cycle set L, the damage of one cycle is determined by the integration areas A1+A2+A3+A4, whereas the damage of the other cycle is determined only by area A4. For cycle set S, the damage of one cycle is determined by the integration areas A2+A4 and the damage of the other cycle is determined by the integration areas A3+A4. Therefore, it is evident that the damage of cycle set L (one with the largest overall range) is relatively larger. The existence or non-existence of a 'cycle set S', which has a smaller damage, serves as the building block of the proof provided in counting method.

3. Crossing-consistent peak count

The relation between level up-crossings and peaks as well as valleys is expressed as follows [2]:

$$\begin{aligned}\#\,\text{level up} - \text{crossings} = {} & \#\,\text{peaks (above that level)} \\ & - \#\,\text{valleys (above that level)}\end{aligned} \tag{8}$$

Between every level up-crossing and the succeeding down-crossing, there always exists one more peak than the number of valleys.[1] Therefore, an obvious choice to make the peak count crossing-consistent is to pair each valley with a peak present immediately above it. Accordingly, the crossing-consistent peak count consists of the following two steps (Fig. 6):

1. Determine all peaks and all valleys.
2. Pair each valley, from the largest one to the smallest, with its closest peak (above that particular valley), with each cycle counted as a full cycle.

[1] The relation can be verified by manually drawing several random signals between an up-crossing and down-crossing.

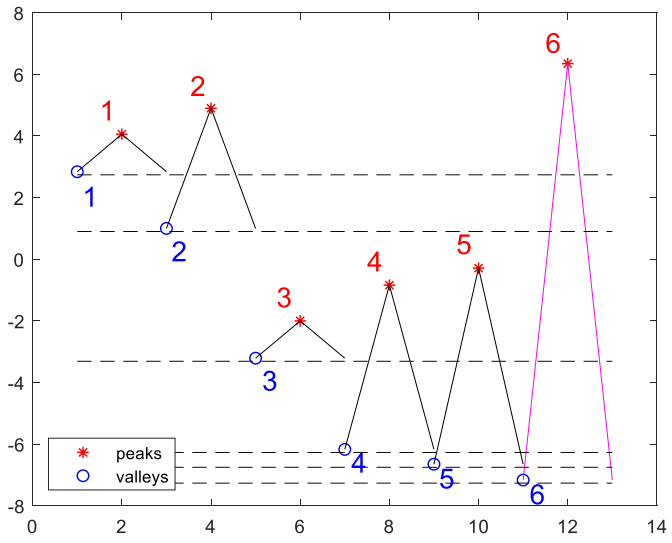

Fig. 7. Cycles obtained using the crossing-consistent peak count (from time series of Fig. 6a).

Fig. 6a shows the same load time series as in Fig. 3a. The load levels were chosen to be immediately below the valleys. The cycles determined by the crossing-consistent peak count, as described above, can be seen in Figs. 6b and 7. For a load signal with a symmetrical density around the mean level, a fraction of the cycles (with positive peaks and negative valleys, marked by magenta in Fig. 7) will be in the vicinity of the green diagonal. The other fraction of cycles (with either positive peaks and positive valleys or negative peaks and negative valleys) will be immediately above the magenta diagonal. The cumulative histogram plotted in Fig. 6c clearly shows that $N(u,u)$ equals the number of up-crossings N_u for each of the six levels.

Notably, unlike other counting methods, the order of the peaks and valleys is irrelevant for the peak count.

4. Proof that the crossing-consistent peak count is the most conservative

Before proceeding to the proof, we must discuss the cumulative histogram.

For the example plotted in Fig. 6, the cumulative histogram K according to Eq. (7) is plotted in Fig. 8. The matrix elements have been determined iteratively, starting with the lowest value on the super-diagonal (shown in red). Based on a given value of the right hand side of Eq. (7), all table cells were placed to the left and above. Consequently, the red shaded rectangular portion in Fig. 8b could be assigned the same value (indicated in red). Next, the super-diagonal value in green was obtained as it had the same magnitude. The empty cells of the green column in Fig. 8c were assigned this particular value. This procedure was repeated until all cells of the super-diagonal were considered. The cumulative histogram obtained as a result is exactly the same as the one obtained for crossing-consistent peak count (see Fig. 6c).

Next, the proof is provided for why this must be the case for any load time series.

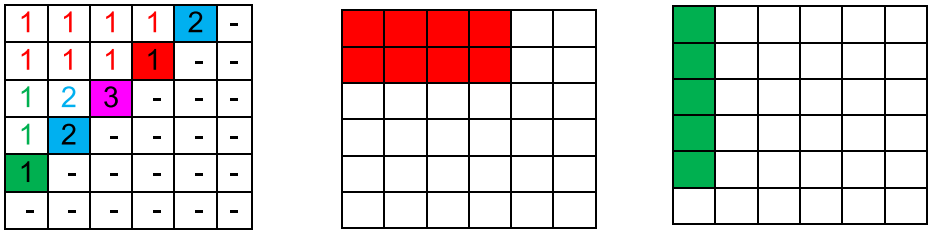

Fig. 8. a) The cumulative histogram $K(u,v)$ of the most conservative cycle count for given N_u, b) Area corresponding with the red shadowed super-diagonal cell, and, c) Area corresponding with the green shadowed super-diagonal cell. (For interpretation of the references to colour in this figure legend, the reader is referred to the Web version of this article.)

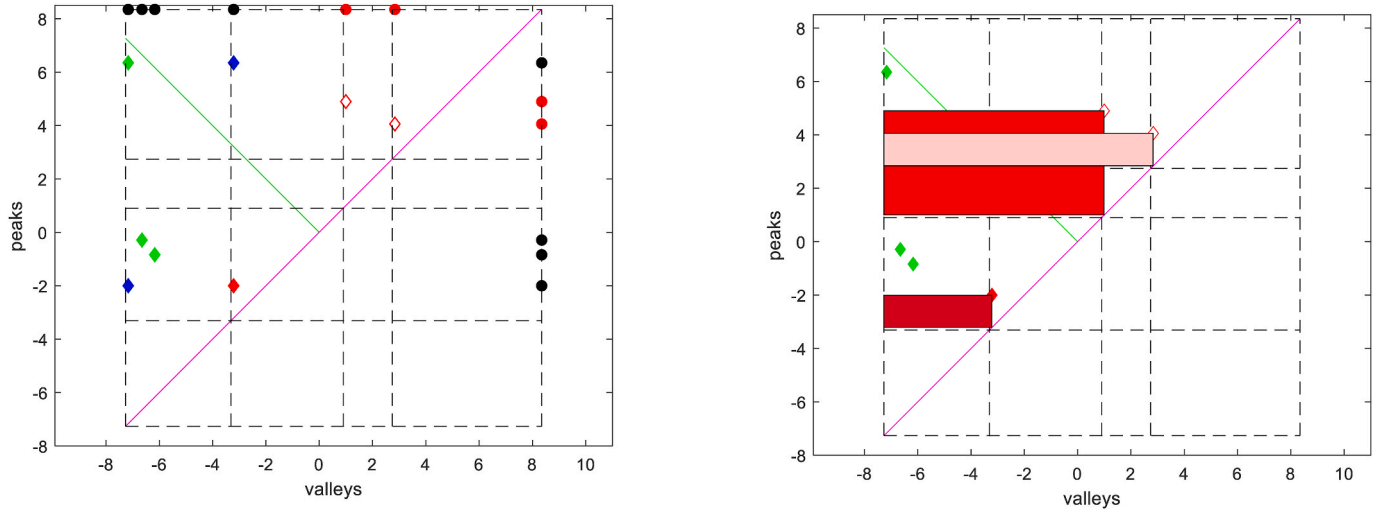

Fig. 9. a) Pairing the 3rd valley to the correct peak according to the crossing-consistent peak count (red filled diamond). Two cycles have already been paired (red open diamonds), implying that four valleys and four peaks (black dots on the top and at the right) are yet to be paired. The two blue filled diamonds indicate possible alternatives. b) The exclusion zones for all cycles following the 3rd cycle. (For interpretation of the references to colour in this figure legend, the reader is referred to the Web version of this article.)

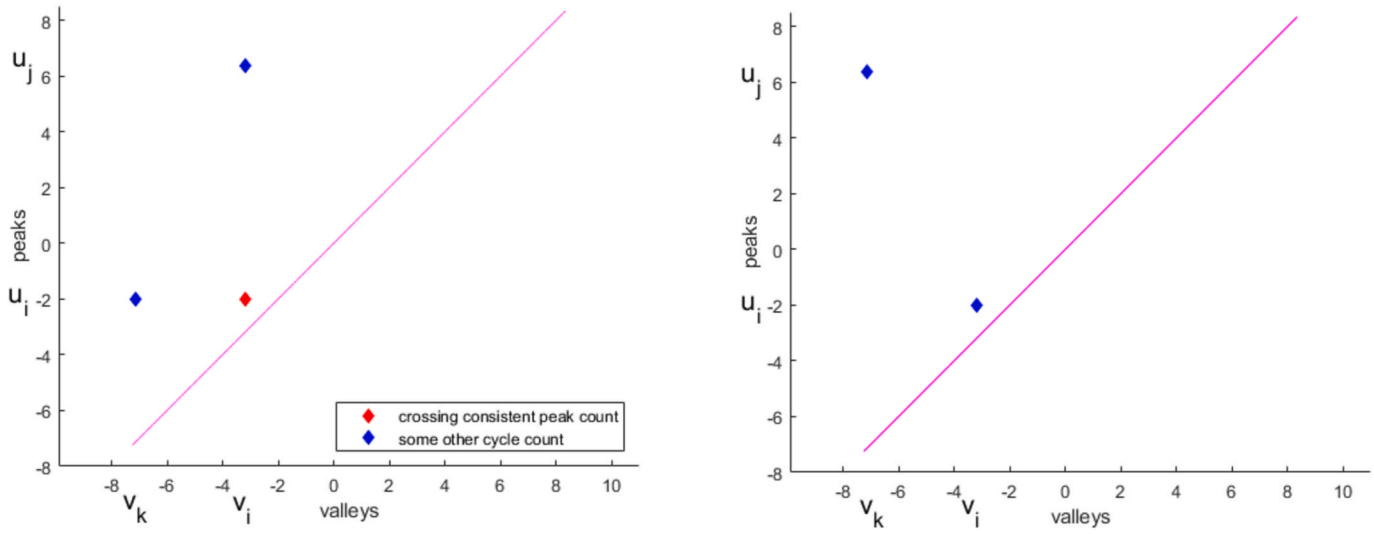

Fig. 10. a) First difference between the crossing-consistent peak count and a different cycle-counting method, b) a more conservative situation (for a different cycle counting method); a 'cycle set L'.

One way to understand cycle-counting methods is that they pair all peaks to the valleys in some order. Theoretically, this can be done in $N!$ ways, where N is the number of valleys. The goal here is to obtain the most conservative cycle-counting method such that no permutation (pairing some peak to another valley) can lead to a higher estimated damage. For this purpose, this study utilised the scenario shown in Fig. 5. For a 'cycle set S', a permutation 'cycle set L' is also possible, showing that the specific count method need not be the most conservative. In particular, 'cycle set S' is expressed as (v_1,u_2) and (v_2,u_1), i.e., the largest peak is paired with the largest valley for one cycle, and for the other cycle, the smallest peak is paired with the smallest valley. Then, the 'cycle set L' is expressed as (v_1,u_1) and (v_2,u_2), where

$$v_2 < v_1 \quad \text{and} \quad u_2 > u_1 > v_1. \tag{9}$$

The condition $u_1 > v_1$ ensures that the cycle lies above the (magenta) diagonal, i.e., it has a positive range. The situation where $u_1 = u_2$ (or $v_1 = v_2$) can be ignored because an exchange does not matter.

Next, the procedure of the crossing-consistent peak count is described. As mentioned, the pairing of the peaks to the valleys is an iterative process. As an example, the situation for the 3rd cycle is shown in Fig. 9, implying that two cycles had already been formed. Following the 2nd step, the third valley was paired with the lowest available peak. For this example, all four remaining peaks were larger than the 3rd valley. This increased its potential to be chosen.

Possible alternatives are indicated by blue diamonds. Next, it will be demonstrated that these possible choices can only lead to a relatively lower fatigue damage. Because the crossing-consistent peak count considers the smallest possible peak, for the ith cycle, none of the remaining cycles can lie inside the area marked by Eq. (10):

$$v < v_i \quad \text{and} \quad v_i < u < u_i \tag{10}$$

In Fig. 9b, these exclusion zones are shaded in red. This implies that the remaining cycles should lie either above or below this exclusion zone, assuring that no 'cycle set S' will be present. In case they lie above it, by applying the terminology of Fig. 5, the next cycle is expressed as (v_2,u_2). It will form a 'cycle set L' with the ith cycle (v_1,u_1) to satisfy Eq. (9). In case they lie below the exclusion zone, the next cycle is expressed as (v_2, u_1) and cannot form a 'cycle set S' with the ith cycle, which is now expressed as (v_1,u_2), because $u_1 < v_1$. Therefore, it is guaranteed that any change in the pairing will lead to a less conservative result.

Another way to look at this problem is to consider other cycle-counting methods and compare them with the crossing-consistent peak count. It will be shown that the application of some other cycle count method will lead to at least one 'cycle set S'. For a different method, the first difference (considering the valleys from the largest to the smallest one) occurs at the ith valley (Fig. 10a). In other words, the paired peak is unequal to u_i (red diamond). Let us instead assume that v_i and u_i are paired with u_j and v_k, respectively (blue diamonds in Fig. 10). Then, $v_k < v_i$ should hold true because the valleys are being considered from large to small amplitudes. Furthermore, $u_j > u_i$ because the crossing-consistent peak count considers the smallest possible peak. Moreover, because it is a cycle, $u_i > v_i$. Thus, all three requirements of Eq. (9) are met, implying that, for any cycle method other than the crossing-consistent peak count, there will be at least one possibility to make it more conservative by switching peaks (Fig. 10b). Therefore, no other cycle method can be the most conservative.

This finalises the proof.

5. Application to stress time series

In this section, the crossing-consistent peak count is applied to various stress time series. In particular, the crossing-consistent peak count is compared with the rainflow count (applying the built-in MATLAB routine *rainflow.m*, based on [4]) as well as the range count (taking all ranges into account, i.e., valleys-to-peaks and peaks-to-valleys). The number of cycles equals (number of reversals - 1)/2. In this case, crossing consistency implies that the super-diagonal of the cumulative histogram equals the mean of the up- and down-crossings. In case of a half cycle, two peaks are paired with one valley (or vice versa). It can be anticipated that the start point as well as the end point of a time series forms half cycles. The flowchart of the rainflow count indicates that this is always the case. At least one more half cycle is required to pair the two reversals that have been paired with the start and end points. Another feature of the rainflow count, which can be deduced from the flowchart,[2] is that the largest possible range, i.e., pairing of the highest peak with the lowest valley, is always included.

Inspired by this the proposed framework can now be expanded to include half cycles:

1. All reversals of the time series are considered twice, except the start and end points.

[2] https://nl.mathworks.com/help/releases/R2023b/signal/ref/rainflow.html.

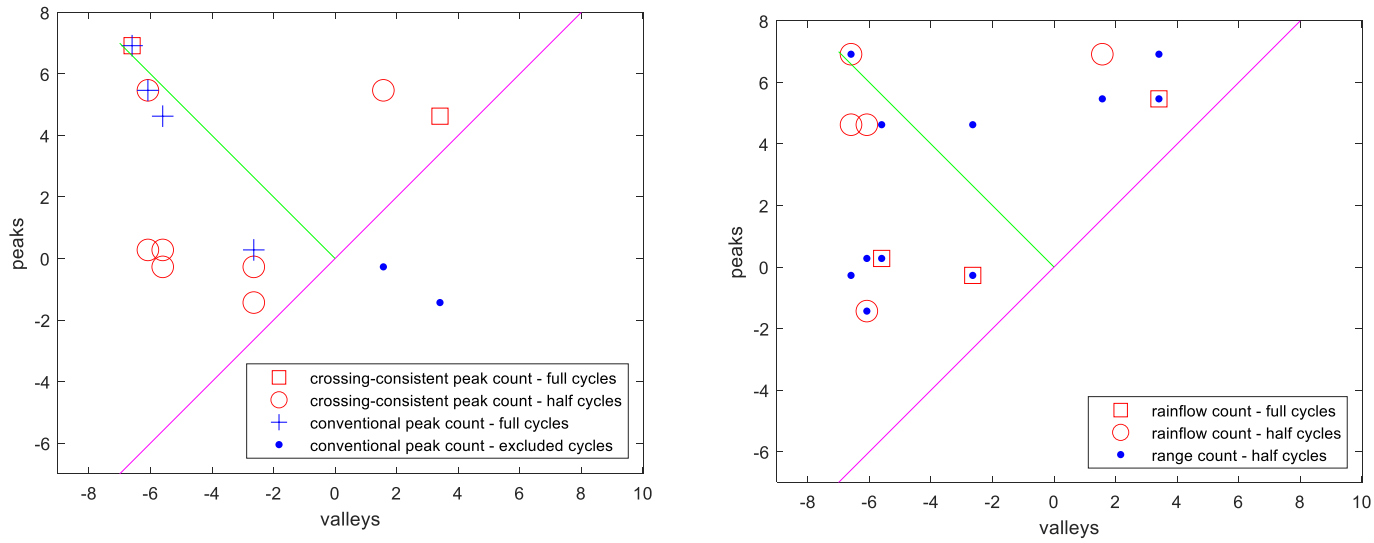

Fig. 11. Scatter plot of the cycles of the example time series (Fig. 3a, with mean subtracted), for several counting methods.

Table 1
Relative fatigue damage (normalised by the fatigue damage measured using rainflow count) of the example time series; $m = 8$.

Time series by figure	Rainflow count	Crossing-consistent peak count	Conventional peak count	Range count
Fig. 1a	1.00	1.25	1.25	0.55
Fig. 2	1.00	1.00	0.36	1.00
Fig. 3a	1.00	1.65	2.01	0.81

smallest valley). According to the two steps of the previous section, the largest of this surplus of peaks will be saved to be paired with the smallest valley. An exception of Eq. (8) is the combined situation in which no down-crossing occurs after the up-crossing, i.e., the time series ends with a valley. In this case, the number of peaks above the level equals the number of valleys. However, because the mirroring happens without the end valley, there will still be one more peak than the number of valleys. Thus, it can be concluded that the largest possible range is always included in the crossing-consistent peak count.

One may question why half cycles should be considered at all. The

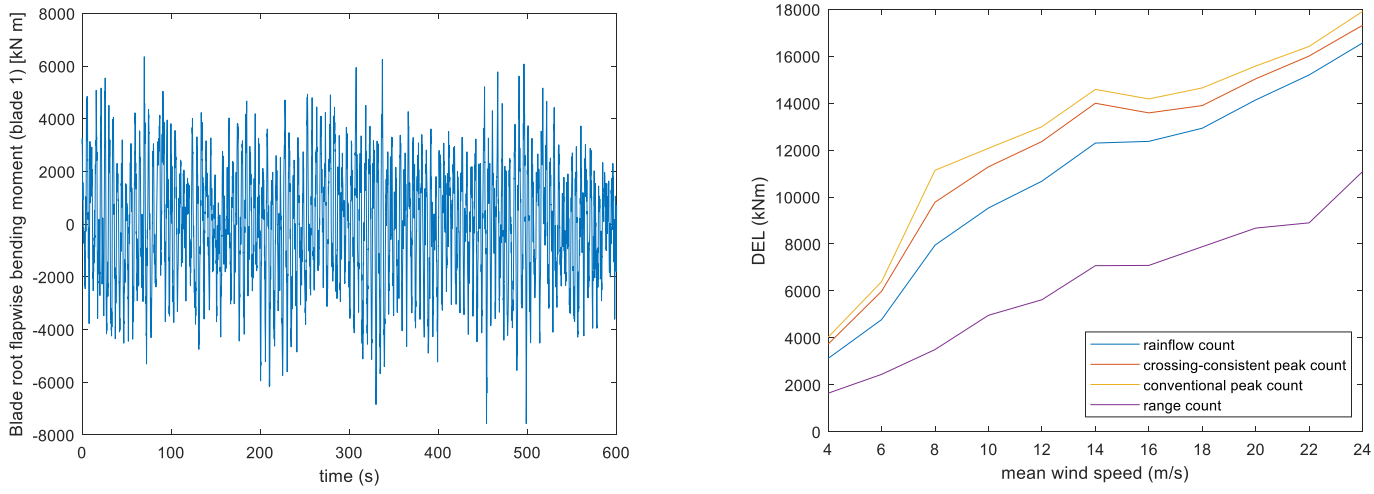

Fig. 12. Blade root flapwise bending moment: a) Time series for a mean wind speed of 24 m/s, and b) comparison of the damage-equivalent load (for $N_{eq} = 1$ and $m = 8$) as function of mean wind speed, for several counting methods.

2. The two steps listed in Section 3 are applied and the obtained cycles are counted as half.
3. Duplicate half cycles are converted into full cycles.

The first step assures that the correct number of cycles is obtained and can be inferred as the mirroring of the time series around the start point (excluding the end point). The symmetry resulting from this mirroring assures that there always exists at least one up-crossing at each level that is considered immediately below the valleys. Therefore, the number of peaks should be greater than the number of valleys above each of these levels by at least one (except for the level below the underlying reason is that, in a finite time series, the largest range, which generally counts as a half cycle, contributes considerably to the overall damage [8].

We applied the updated procedure to our example load time series and compared it to other cycle count methods (see Fig. 11 and Table 1). As shown, the conventional peak count is not crossing-consistent because it leads to cycles having a negative stress range.

The remainder of this section discusses the analysis of realistic loads. Because the current author is member of the Wind Energy group at TU Delft, to demonstrate the practical application of this approach, only wind turbine loads are considered. However, it should be noted that this

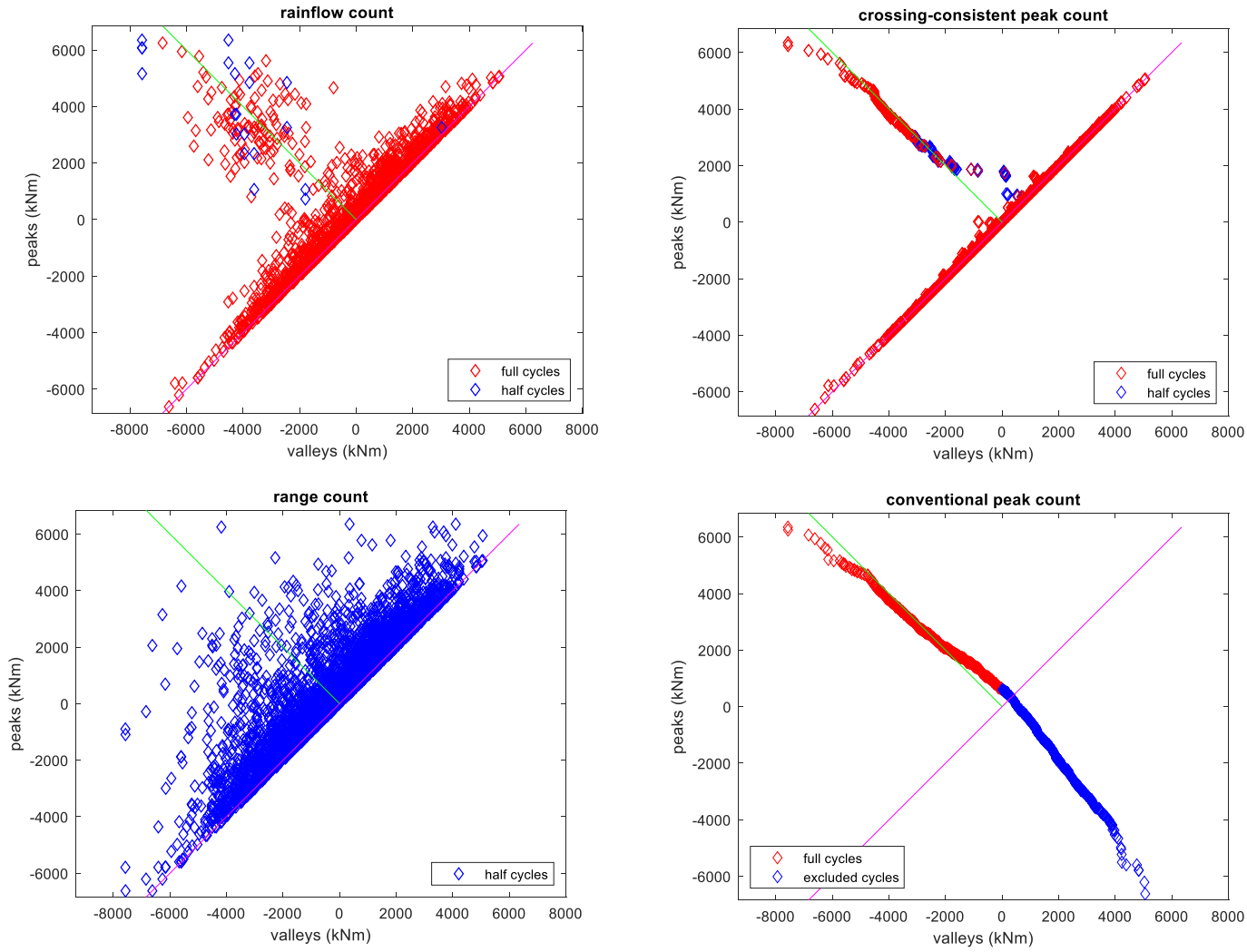

Fig. 13. Scatter plots obtained by applying different counting methods to the cycles measured for the blade root flapwise bending moment (mean wind speed = 24 m/s).

approach is applicable to any other load type. Time-series data were acquired using the FAST package, and NREL's primary physics-based engineering tool was used for simulating the coupled dynamic response of wind turbines. The reference NREL 5 MW turbine [9] was used in this study. As is common for the fatigue analysis of wind turbines, 10-min time series were considered by first simulating the 11-min time series followed by ignoring the first minute (with respect to transient response). Typically, the loads at specific locations and directions are also considered. This study focuses on the blade root flapwise[3] and edgewise moments, which occur in the wind direction and in the plane of rotation, respectively. In Fig. 12, the comparison between several counting methods is shown. In the wind energy industry, the rainflow count is applied by default. For practical reasons, the damage-equivalent load *DEL* (Eq. (11)) is shown instead of the damage.

$$DEL = \left(\frac{\sum_{i=1}^{N} L_i{}^m}{N_{eq}} \right)^{\frac{1}{m}}, \tag{11}$$

where N_{eq} *is* the equivalent number of cycles and L denotes the load range.

In Fig. 13, the corresponding scatter plots are plotted for a single mean wind speed. The edgewise moment is dominated by the gravity load, leading to an almost perfect sinusoid (see Fig. 14a), with a small ripple at its top (only visible when the plot is enlarged), due to the aerodynamic forces. This yields a distinct scatterplot shown in Fig. 14b.

The Appendix of this paper details how that the mean damage of a Gaussian process according to the crossing-consistent peak count is equal to the narrow-band approximation of fatigue damage. The wind turbine loads cannot be utilised to demonstrate this because they are typically not Gaussian. However, wind turbine loads are outputs of the simulation software, which accepts wind fields that resemble atmospheric turbulence as its inputs. These wind fields are generated via summation of numerous harmonics with random phases and amplitudes based on the spectrum of turbulence (using the Kaimal spectrum). Therefore, it is implicitly assumed that they are Gaussian. For Fig. 15, 100 time series of these wind fields measured for 10-min each (totalling to approximately 17 h) were used.

From the Kaimal spectrum, the regularity factor α for the wind fields can be determined to be ~ 0.1. Based on Eq. (A.1), this implies that the number of cycles near the $y = -x$ diagonal is approximately 10% of the total number of cycles. The distribution of these cycles is an approximately Rayleigh distribution, as shown in Fig. 15c. Note that the

[3] Because wind turbine blades are made of composite material, the mean value per cycle should in fact also be included in the damage calculation. Since the fatigue framework developed at the Lund University is based on Eq. (1) , all damages are presented accordingly, thus without mean value correction.

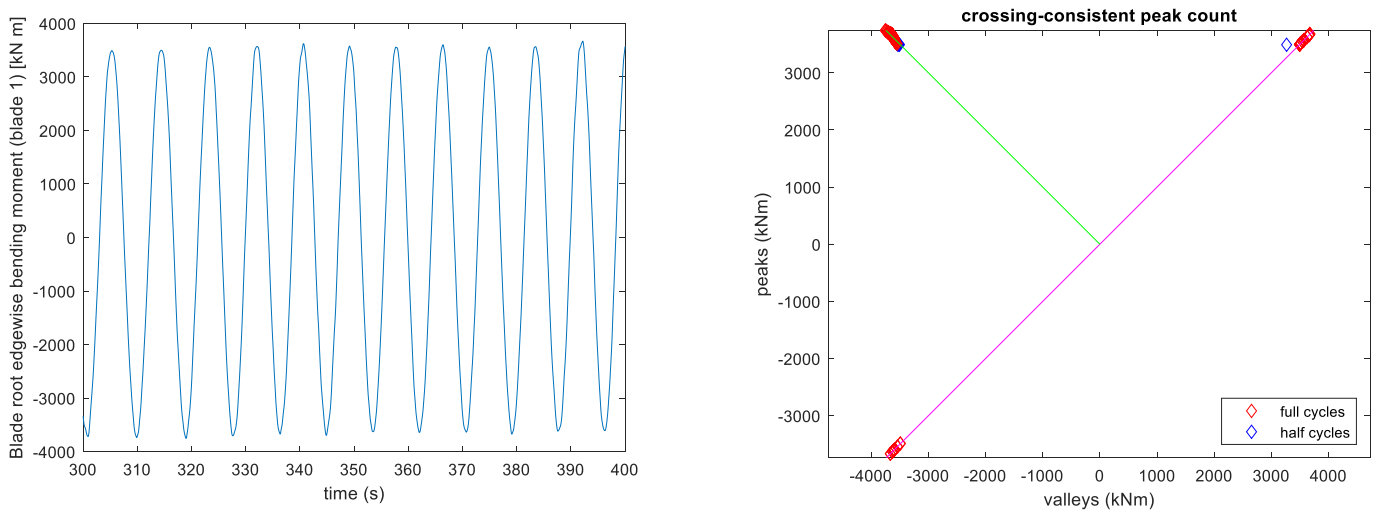

Fig. 14. Blade root edgewise bending moment (mean wind speed = 4 m/s). a) Partial graph of the time series, b) scatter plot of the cycles according to the crossing-consistent peak count.

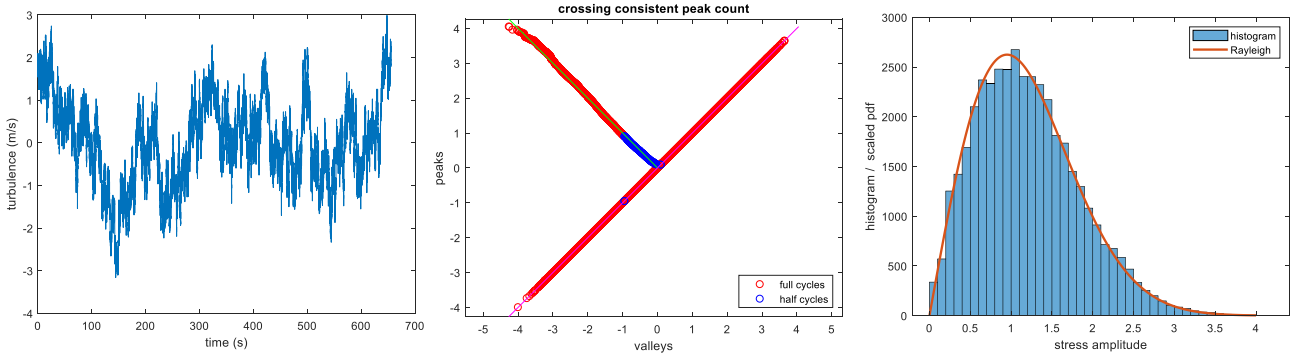

Fig. 15. Gaussian time series: a) Example time series of turbulent wind (around a mean wind speed of 13 m/s); b) scatter plot of the cycles according to the crossing-consistent peak count; and c) comparison of the histogram of the amplitudes and the Rayleigh density (with scale factor equal to the standard deviation of the signal).

amplitudes of the cycles near the $y = x$ diagonal are too small and, thus, were omitted in the graph. It can be concluded that, the crossing-consistent peak count for long time series asymptotically approaches a Rayleigh distribution for the cycles. Due to the increased number of peaks, the next peak to be chosen, i.e., the peak immediately above a particular valley, will get increasingly closer to that valley (and asymptotically approaches the y = x diagonal). At some moment, for negative valleys, no nearby peak will be available. In that case, a peak of approximately the same absolute magnitude (but opposite sign) is chosen instead. Such a cycle will end up closer to the y = -x diagonal. This process is continued until the smallest valley is paired with the largest peak. This implies that the mean damage of the crossing-consistent peak count is given by the narrow-band approximation expressed in Eq. (A.7).

6. Conclusion and outlook

In this work, a variant of the peak count, termed the crossing-consistent peak count, is proposed. In this counting method, valleys are paired, from the largest to the smallest, with their closest peak. Using the fatigue framework developed by the Lund University, this study proves that this counting method is the most conservative of all crossing-consistent counts. This is valid for all time series, i.e., it is not restricted to the Gaussian signals.

In addition to its theoretical significance, the crossing-consistent peak count can be of practical interest. For example, in Ref. [8], an easy approach to check a rainflow count calculation is proposed. This approach is similar to those based on the upper bound given by the narrow-band approximation. Because the upper bound refers to the mean damage, it will not necessarily hold for every stress time series. For scenarios that require absolute certainty, the crossing-consistent peak count can be applied.

The proposed counting method can also be used to invalidate rainflow count routines, for example, the algorithm developed by Gong.[4] For a stress time series equal to [8; 6;3; 2;5; 10; 10; 7;5; 6;7; 8;10; 8;4; 2;3; 6;0;-10], which is identical to the example mentioned in the comment lines of that routine (except that one '10' is added), this routine leads to a damage at m = 8, which is more than four orders smaller than according to the peak count, implying that the routine is invalid.

The crossing-consistent peak count can be used as a reference [10], because it is a counting method applicable to a finite time series, and is closest to the narrow-band approximation. Equivalently, the ranges from the crossing-consistent peak count are closest to Rayleigh.

Declaration of competing interests

The authors declare that they have no known competing financial interests or personal relationships that could have appeared to influence

[4] https://www.mathworks.com/matlabcentral/fileexchange/38834-simple-rain-flow-counting-algorithm.

the work reported in this paper.

Acknowledgement

The author is grateful to Mikael Abrahamsson (Library of Mathematics, Lund University) for providing a copy of [6] for this study.

Appendix. The mean damage of a Gaussian process according to the peak count

For completeness, the result obtained in Ref. [2] with respect to the peak count of a stationary Gaussian process (with zero mean) is repeated in this appendix. For an infinitely long time series, all positive valleys can be paired with positive peaks of equal magnitude, leading to cycles of zero range. Similarly, all negative peaks can be paired with negative valleys of equal magnitude, leading again to cycles of zero range. Thus, these cycles can be ignored, leaving only the positive peaks in the green shaded area in the graph below. As mentioned earlier, the number of level up-crossings equals the number of peaks above that level minus the number of valleys above that level. Application to the mean level, results into the following[5]:

$$N_0 = N_{p+} - N_{v+} = \alpha N_p, \tag{A.1}$$

where $\alpha = N_0/N_p$ is the regularity factor. The remaining positive peaks, which thus form a fraction α of the total number of peaks, are paired with negative valleys of equal absolute magnitude, as schematically indicated in Fig. A1. The above reasoning also holds for the crossing-consistent peak count.

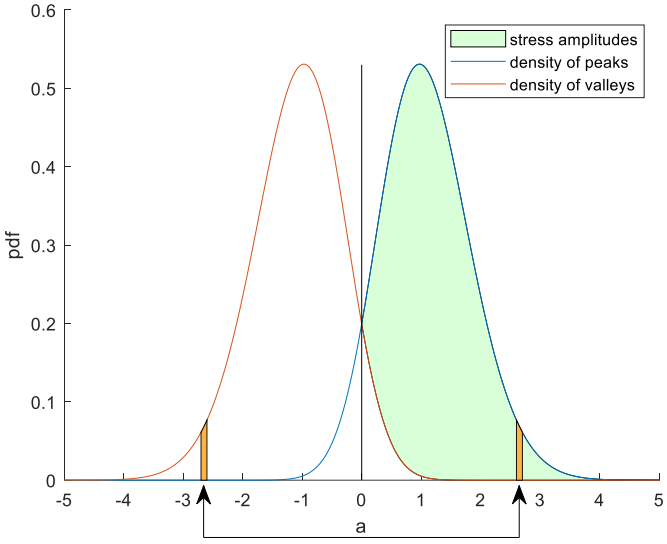

Fig. A1. The peak count (based on [2]).

For a Gaussian process, the density of peaks u is given by the Rice expression [11] (with bandwidth parameter $\delta = \sqrt{1-\alpha^2}$):

$$f_p(u) = \frac{\sqrt{1-\alpha^2}}{\sigma}\varphi\left(\frac{1}{\sigma\sqrt{1-\alpha^2}}u\right) + \frac{\alpha}{\sigma^2}ue^{-\frac{u^2}{2\sigma^2}}\Phi\left(\frac{\alpha}{\sigma\sqrt{1-\alpha^2}}u\right), \tag{A.2}$$

where, σ is the standard deviation of the stress signal and ϕ and Φ denote the standard normal density and distribution function, respectively. Similarly, for valleys v, the density is expressed as follows:

$$f_v(v) = \frac{\sqrt{1-\alpha^2}}{\sigma}\varphi\left(\frac{1}{\sigma\sqrt{1-\alpha^2}}v\right) - \frac{\alpha}{\sigma^2}ve^{-\frac{v^2}{2\sigma^2}}\Phi\left(-\frac{\alpha}{\sigma\sqrt{1-\alpha^2}}v\right). \tag{A.3}$$

Fig. A1 shows that the density of the amplitude a of the cycles of a peak count is obtained by subtracting the densities of the valleys from the density of peaks and next normalisation given as follows:

$$f_c(a) = \frac{1}{\alpha}\left(f_p(a) - f_v(a)\right). \tag{A.4}$$

Substitution of Eq. (A.2) and (A.3) leads to the following:

[5] There is an inconsistency in Ref. [2]: In Section 9.2.2 it is stated that 'In the peak count, all local maxima above zero are counted'. In this paper, the author indicates that counting method as 'the conventional peak count'. This obviously deviates from the peak count visualised by Fig. A1. This implies that the average damage from a conventional peak count will be above the narrow-band expression. Refer to the dashed line in Fig. 6.3 in Ref. [3].

$$f_c(a) = \frac{1}{\alpha}\left(\frac{\alpha}{\sigma^2} a e^{-\frac{a^2}{2\sigma^2}}\left(\Phi\left(\frac{\alpha}{\sigma\sqrt{1-\alpha^2}}a\right) + \Phi\left(-\frac{\alpha}{\sigma\sqrt{1-\alpha^2}}a\right)\right)\right) = \frac{a}{\sigma^2} e^{-\frac{a^2}{2\sigma^2}}. \tag{A.5}$$

By utilising a symmetry property of the standard normal distribution function around $\Phi(0) = 0.5$, the derivation holds for any value for α. Hence, it is valid for broad band signals as well. Therefore, a Rayleigh density is obtained with scale parameter σ. Note that the density of the cycle amplitudes is not dependent on some bandwidth parameter.

An alternative way to derive Eq. (A.5) is as follows: the surplus of positive peaks above some level a, which can consequently be paired with negative valleys, is equal to the number of up-crossings of that level (Eq. (8)). According to Rice, the number of up-crossings above level a is given by the following equation:

$$N_0 e^{-\frac{a^2}{2\sigma^2}}. \tag{A.6}$$

This indeed corresponds to the exceedance probability $Q=1-F$ of a Rayleigh distribution with scale parameter σ.

Therefore, the mean damage of a Gaussian process, according to the peak count, equals the mean damage of an equivalent narrow-band process, given as follows:

$$\overline{D}_{NB} = \frac{N_0}{K}\left(2\sqrt{2}\sigma\right)^m \Gamma\left(1+\frac{m}{2}\right). \tag{A.7}$$

This implies a narrow-band process with standard deviation σ and N_0 number of zero-up-crossings.

In [2], this statement about the peak count is made: '*The number of stress cycles is thereby reduced but larger weights are given to large stress ranges, so although no rigorous proof is given, the procedure is expected to result in estimates of damages larger than the actual values*'. As mentioned, in Ref. [7] a strict mathematical proof is given that this narrow-band approximation forms an upper bound of the mean damage of any crossing-consistent counting method.

Data availability

Data will be made available on request.

References

[1] T. Dirlik, D. Benasciutti, Dirlik and Tovo-Benasciutti spectral methods in vibration fatigue: a review with a historical perspective, Metals 11 (9) (2021), https://doi.org/10.3390/met11091333.

[2] H.O. Madsen, S. Krenk, N.C. Lind, Methods of Structural Safety, Dover, 1986/2006.

[3] I. Rychlik, S. Gupta, G. Lindgren, Fatigue Prediction for Random Loads Using the Rainflow Method, CRC press, 2025, https://doi.org/10.1201/9781003019947.

[4] ASTM. Standard practices for cycle counting in fatigue analysis. https://www.astm.org/e1049-85r17.html.

[5] I. Rychlik, Note on cycle counts in irregular loads, Fatig. Fract. Eng. Mater. Struct. 16 (4) (1993) 377–390, https://doi.org/10.1111/j.1460-2695.1993.tb00094.x.

[6] M. Frendahl, I. Rychlik, Rainflow analysis – Markov method. Stat Res Report 1992: 6 (Dept of Mathematical Statistics, University of Lund, 1992, pp. 1–60.

[7] I. Rychlik, On the "narrow-band" approximation for expected fatigue damage, Probab. Eng. Mech. 8 (1993) 1–4, https://doi.org/10.1016/0266-8920(93)90024-P.

[8] W. Bierbooms, An Easy Approach to Check for Order Size of a Time Domain Fatigue calculation- Rainflow Counting Revisited, To Be Published, 2026.

[9] J. Jonkman, S. Butterfield, W. Musial, G. Scott, Definition of a 5-MW Reference Wind Turbine for Offshore System Development, National Renewable Energy Laboratory, 2009, https://doi.org/10.2172/947422. Technical report no. NREL/TP-500-38060.

[10] W. Bierbooms, How to check a time domain fatigue calculation via 4 simple hand calculations, J. Phys.: Conf. Ser.,Sci.Making Torque from Wind (2026).

[11] W. Bierbooms, D. Veldkamp, Probabilistic treatment of IEC 61400-1 standard based extreme wind events, Wind Energy 27 (11) (2024) 1319–1339, https://doi.org/10.1002/we.2914.